Journal of Applied Polymer Science

Artificial weathering effect on the structure and properties of polypropylene/polyamide-6 blends compatibilized with PP-*g*-MA

Samir Mouffok,[1] Mustapha Kaci[2]
[1]Laboratoire de Traitement et Mise en Forme des Polymères, Université M. Bougara, Boumerdès Algeria
[2]Laboratoire des Matériaux Polymères Avancés (LMPA), Université A. Mira, Bejaia 06000, Algeria
Correspondence to: S. Mouffok (E-mail: mouffoks@hotmail.com)

ABSTRACT: The degradation of uncompatibilized and compatibilized PP/PA-6 (70/30 wt %) with PP-*g*-MA under accelerated UV light was investigated using Fourier Transform Infrared Spectroscopy (FTIR) spectroscopy, melt flow index (MFI) tester, tensile test, differential scanning calorimetry (DSC), thermogravimetric analysis (TGA) and scanning electron microscopy (SEM). FTIR analysis of the structure of the compatibilized and uncompatibilized blends after exposure to UV light showed the formation of photoproducts corresponding to both components. The MFI and mechanical results obtained revealed that photooxidation started primarily in PA-6 rather than PP. In addition, the uncompatibilized blends exhibited a higher degradation rate compared to neat polymers for long exposure time, and the addition of PP-*g*-MA increased slightly their ageing rate in accordance with TGA data. Further, DSC analysis showed an increase in the crystallinity index and a decrease in the melting temperature of PP and PA-6 after UV exposure either as neat polymers or as blend components. SEM micrographs of the cryo-fractured surfaces of the samples illustrated the formation of cracks and fractures after UV irradiation. © 2014 Wiley Periodicals, Inc. J. Appl. Polym. Sci. **2015**, *132*, 41722.

KEYWORDS: blends; compatibilization; degradation; mechanical properties; thermal properties

Received 20 July 2014; accepted 3 November 2014
DOI: 10.1002/app.41722

INTRODUCTION

Polymer blends based on polypropylene (PP) and polyamide-6 (PA-6) are of great interest owing to their excellent mutually compensating properties. Blending the two polymers can combine their advantages and overcome some of their drawbacks.[1,2] Unfortunately, the two polymers are immiscible and their blends lead to macro-phase separation and consequently to a material of poor properties. The miscibility of the two components may be improved by the addition of a suitable compatibilizer. In fact, when a compatibilizer is added to an immiscible polymer mixture, the blend exhibits finely dispersed morphology and phase stability.[1,3]

The study of degradation and stabilization of polymers is extremely important from the scientific and industrial point of view, to insure a long service life of the product. Chemical degradation of polymers is an irreversible change and is a very important phenomenon, which affects their performances in daily life and leads finally to the loss of functionality.[4] Photooxidative degradation is the process of decomposition of the material by the action of light, which is considered as one of the primary sources of damage of polymeric substrates in ambient conditions. The most damaging effects are the visual effect (yellowing), the loss of mechanical properties of the polymers, the changes in molecular weight and the molecular weight distribution.[5] Polymer blend degradation is a very complex phenomenon due to the variety of interactions between the blend components. These may generate antagonistic or synergistic effects, depending on the composition, the degradation conditions and the blend miscibility.[6] Some synergistic effects include: prodegrading species generated in a domain migrating to another domain, which would change the degradation kinetics, and different domains degrading independently without variation in degradation kinetics of the blend components.[7] This means that individual component of a blend may behave rather differently from their behavior as isolated polymers, affecting thus the overall degradation resistance positively or negatively. The processes are more complicated in the presence of compatibilizers. Consequently, it is difficult to predict the degradation behavior of polymer blends without experiments.[8,9]

Extensive work has been devoted on the elaboration and characterisation of PP/PA-6 blends.[2,3,10–14] However, in spite of the considerable work carried out on the degradation of neat polymers,[6,15] there are only a few papers which deal with their ageing, and more particularly with the ultraviolet (UV) photodegradation in the presence of a compatibilizer. A previous work was carried out on the influence of natural weathering on the physical properties of PP/PA-6 blends.[16] So far, this study did not deal with the effect of

the compatibilizer on their degradation rate. The results obtained did not show important changes in the chemical structure of the compatibilized blends compared to the uncompatibilzed ones after one year of outdoor exposure. Other works carried out on the photooxidation of the compatibilized polypropylene (PP)/polystyrene (PS) blend revealed that the compatibilizer acts as a photodegradation promoter of the blend.[6]

Therefore, the present work is aimed to investigate the accelerated UV ageing effect on the structure, the morphology, the thermal and the mechanical properties of PP/PA-6 (70/30 wt %) blends compatibilized with the maleic anhydride grafted polypropylene (PP-*g*-MA). The degradation state of the exposed samples is evaluated as a function of exposure time using several techniques Fourier Transform Infrared Spectroscopy (FTIR) spectroscopy, MFI, Tensile test, DSC, thermogravimetric analysis (TGA), and SEM.

EXPERIMENTAL

Materials

The PP used is an isotactic homopolymer produced by INEOS Olefins and Polymers Europe (United Kingdom), under the trade name 100-GA03. PP has a melt flow index (MFI) of 3 g/10 min (at 230°C, load 2.16 kg). PA-6 was supplied by Lanxess (Germany) under the trade name Durethan B 30 S**.** The polymer has an average molecular weight (M_n) = 20,000 g mol^{-1}, a density of 1.14 g cm^{-3}, a water absorption = 10 wt % and a moisture absorption at equilibrium = 3 wt %. The compatibilizer used was PP-*g*-MA from Dupont International S.A. (Australia) under the trade name Fusabond ^{R}P M613-05. The maleic anhydride content is <0.1 wt %. The main characteristics of the compatibilizer are a MFI of 120 g/10 min, a melting temperature of 162°C and a decomposition temperature higher than 250°C.

Specimen Preparation

Melt compounding of PP/PA-6 blends was performed on a Bauzano Counter rotating twin screw extruder (L/D = 19), Italy. The temperature setting along the zones of the extruder was 240°C, whereas the screen rotation speed was 40 rpm. Prior to extrusion, PA-6 pellets were dehumidified in a Moton MDE 40 Desiccant dryer at 90°C for 3 h. All the blend components, that is, PP, PA-6, and PP-*g*-MA were blended together before introduction into the hopper of the extruder. The designation and composition of the blends are given in Table I. The extrudates were pelletized and compression molded at 240°C, under a pressure of 110 MPa into specimens as thin films of about 100 μm.

Artificial Accelerated Photooxidation Test

The compression molded specimens were exposed to accelerated UV test in a Xenon artificial weathering system (Heraeus, Germany) equipped with a filtered Xenon lamp with the irradiation dose of 90 W m^{-2}, ($\lambda > 300$ nm) for a period of 250 h, at 45°C, and in the presence of air.

Characterization Methods

Fourier Transform Infrared Spectroscopy. Infrared spectra were recorded using a Perkin-Elmer, type Spectrum one spectrometer with 4 cm^{-1} resolution and 40 scans. All spectra were recorded in the absorbance mode in the 4000–600 cm^{-1} region.

Table I. Designation and Composition of the Samples

Designation	PP (wt %)	PA-6 (wt %)	PP-*g*-MA (wt %)
PP	100	0	0
PA-6	0	100	0
PP/PA-6/0C	70	30	0
PP/PA-6/2C	68	30	2

Melt Flow Index. The MFI of PP/PA-6 blends before and after exposure to artificial weathering was measured using a Davenport MFI-10 melt flow indexer-Lloyd Instruments, England, at 240°C and 2.16 kg load. Five independent experiments of each sample were realized. The values were checked for consistency and the average values were reported.

Tensile Test. Tensile tests were carried out on both non-irradiated and UV-irradiated samples using a Zwick/Roell Z 250 machine at 23°C, according to ISO 527-3, with a crosshead speed of 50 mm min^{-1}. Prior to testing, all specimens except PP ones were dried at 90°C for 3 h. Tensile strength and percent elongation at break were determined from the stress-strain data. Ten specimens of each sample were tested. The values were checked for consistency and the average values were reported.

Differential Scanning Calorimetry (DSC). DSC analysis was carried out using a Setaram DSC 331 evo DSC. The samples were heated from 25 to 250°C in nitrogen atmosphere. To eliminate the thermal history effect, the first cooling, and the second heating thermograms were recorded with a scanning rate of 20°C min^{-1}. The melting peak (T_m) was obtained, and the crystallinity index (X_c) was calculated as the ratio of the melting enthalpies subdivided by the weight fraction (w_i) of the respective component in the blend,[2] according to eq. (1):

$$X_c = \frac{\Delta H}{w_i . \Delta H_0} \quad (1)$$

where ΔH_0 is the melting enthalpy of 100% crystalline polymer. $\Delta H_{0\,(PP)}$ = 209 J g^{-1} and $\Delta H_{0\,(PA\text{-}6)}$ = 229.9 J g^{-1}.[2]

Thermogravimetric Analysis (TGA). TG experiments were carried out by a NETZSCH STA 409 PC/PG thermal analyser using a scanning rate of 20°C min^{-1} under nitrogen atmosphere in the temperature range starting from 25 to 550°C.

Scanning Electron Microscopy (SEM). The effect of artificial accelerated weathering on the morphology of PP/PA-6 blends was observed with a JEOL JSM 6360LV, SEM operated at 15 kV. SEM micrographs were taken from fractured surfaces of samples after submersion in liquid nitrogen. Prior to observation, the fractured surfaces were coated with a thin gold layer.

RESULTS AND DISCUSSION

FTIR Analysis

The changes in the chemical structure of PP, PA-6, PP/PA-6/0C, and PP/PA-6/2C were examined by FTIR spectroscopy before and after exposure to UV light. No important changes were observed in the region 600–1600 cm^{-1} for all the samples. In

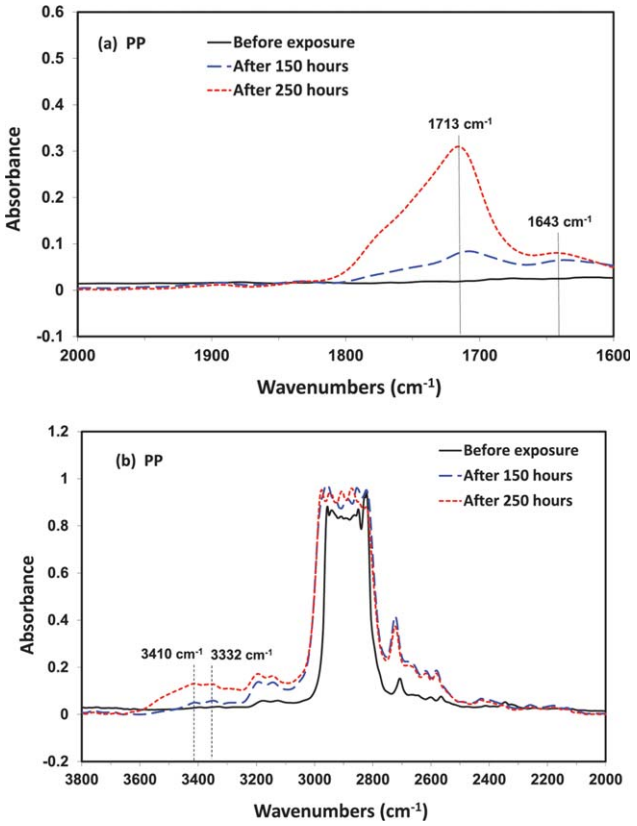

Figure 1. FTIR spectra of PP before and after 150 and 250 h of exposure to artificial weathering: (a) 1600–1900 cm^{-1} and (b) 2000–3800 cm^{-1}. [Color figure can be viewed in the online issue, which is available at wileyonlinelibrary.com.]

details, Figure 1(a,b) shows the FTIR spectra of PP, recorded in the regions of 1600–2000 $cm^{-1}$and 2000–3800 cm^{-1}, respectively, before and after exposure to accelerated UV test for 150 and 250 h. In the region 1600–2000 cm^{-1}, the FTIR spectra show the appearance of new absorption bands at 1643 and 1713 cm^{-1} after 150 h of exposure corresponding to the formation of vinyl groups and carboxylic acids, respectively.[17] The band intensities increase with the exposure time. In the region 2000–3800 cm^{-1}, it is also observed the appearance of a large absorption band centred at 3410 and 3332 cm^{-1} corresponding to hydrogen-bonded hydroperoxides. The intensity of this band increases with the increase of exposure time. The two bands at about 3190 cm^{-1} are referred to the neat PP before exposure. According to Rivaton *et al.*,[18] the mechanism by which the photooxidation occurs in PP involves an induced oxidation of the tertiary carbon atoms that accounts for the formation of tertiary hydroperoxides which can further decompose to carbonyl products.

For PA-6, the infrared spectra recorded in the regions 1600–2000 cm^{-1} and 2000–3800 cm^{-1} are illustrated in Figure 2(a,b), respectively, before and after 150 and 250 h of UV exposure. In the region 1600–2000 cm^{-1}, the FTIR spectra of the irradiated samples exhibit a new absorption band at 1671 cm^{-1} assigned to vinyl groups and the formation of a shoulder at about 1736 cm^{-1} corresponding to imides. However, in the region 2000–3800 cm^{-1}, the FTIR spectra of irradiated samples show the presence of two shoulders in the hydroxyl region whose intensity appears to increase with increasing the exposure time, showing maxima at about 3480, 3365, and 3247 cm^{-1}. The shoulder having a maximum about 3180 cm^{-1} is referred to the neat PA-6 before exposure. Indeed, Lemaire *et al.*[19] suggested that the radical attack on the polyamide backbone occurs at the N-vicinal methylene groups —CONH—CH_2—, and it leads to the formation of imides, hydroperoxides, and N-1 hydroxylated groups.

The FTIR spectra of uncompatibilized PP/PA-6 blends before and after 150 and 250 h of exposure to artificial weathering recorded in the regions of 1600–1900 cm^{-1} and 2000–3800 cm^{-1} are shown in Figure 3(a,b), respectively. The overall spectra after exposure reveal the formation of various absorption bands and shoulders, corresponding to the photoproducts produced by both homopolymers, that is, PP and PA-6 which increase in intensity with the exposure time. Indeed, after exposure to UV light, the FTIR spectra of the irradiated samples recorded in the region 1600–1900 cm^{-1} exhibit new absorption bands at 1647 and 1671 cm^{-1} assigned to vinyl groups and the formation of a shoulder at about 1713 cm^{-1} attributed to carboxylic acids and another one at about 1735 cm^{-1} corresponding to imides. Furthermore, in the region 2000–3800 cm^{-1}, there is a formation of new absorption bands in the hydroxyl region. After the addition of PP-*g*-MA, The FTIR spectra of the

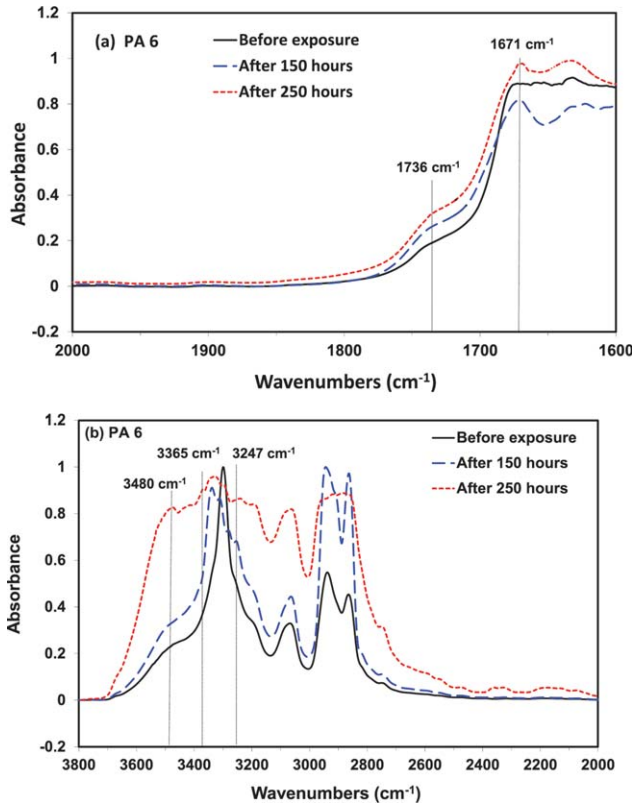

Figure 2. FTIR spectra of PA-6 before and after 150 and 250 h of exposure to artificial weathering: (a) 1600–1900 cm^{-1} and (b) 2000–3800 cm^{-1}. [Color figure can be viewed in the online issue, which is available at wileyonlinelibrary.com.]

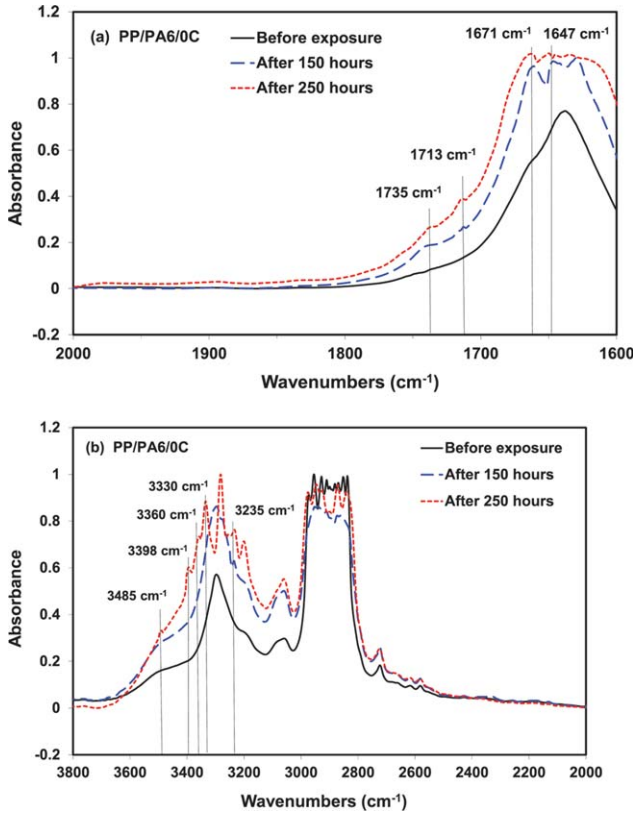

Figure 3. FTIR spectra of PP/PA-6/0C before and after 150 and 250 h of exposure to artificial weathering: (a) 1600–1900 cm^{-1} and (b) 2000–3800 cm^{-1}. [Color figure can be viewed in the online issue, which is available at wileyonlinelibrary.com.]

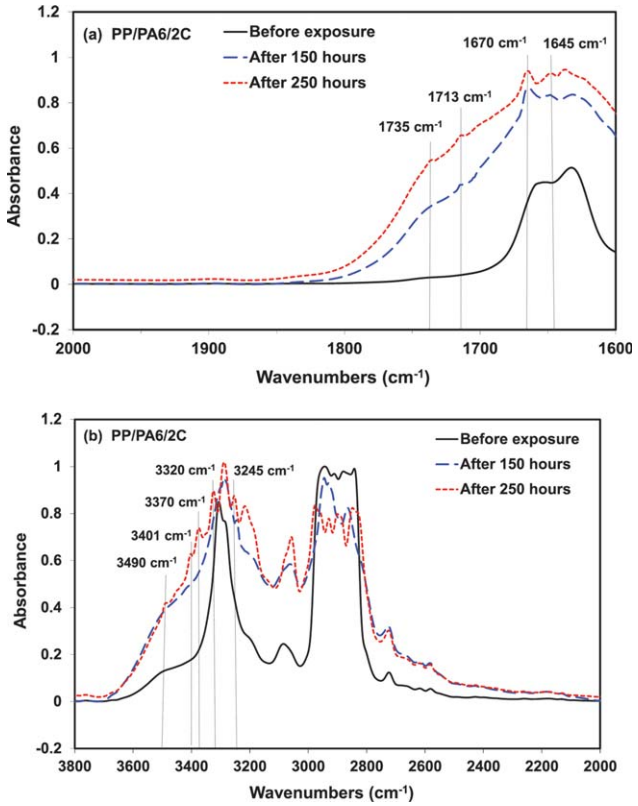

Figure 4. FTIR spectra of PP/PA-6/2C before and after 150 and 250 h of exposure to artificial weathering: (a) 1600–1900 cm^{-1} and (b) 2000–3800 cm^{-1}. [Color figure can be viewed in the online issue, which is available at wileyonlinelibrary.com.]

compatibilized blend samples illustrated in Figure 4(a,b) do not show important changes in the chemical structure comparing to the uncompatibilized ones. However, they exhibit higher band intensities in the carbonyl region, indicating higher degree of photooxidative degradation, which is promoted by the compatibilizer.

Melt Flow Index

The melt flow rate test is a simple and convenient method for characterizing both the mechanism of degradation (chain scission or crosslinking) and the extent of degradation of a polymer since the MFI is inversely related to the molar mass of the polymer and is indicative of the flow characteristics of the molten polymer.[20] In Figure 5, the dimensionless MFI is reported as a function of exposure time. The dimensionless values are calculated by dividing the values of MFI of unexposed samples [$MFI_{(to)}$] by the corresponding values at a given irradiation time [$MFI_{(t)}$]. This means that the lower is the dimensionless MFI, the higher is the extent of degradation. It is observed that this value for the two homopolymers PP and PA-6 decreases slowly up to 100 h of exposure with a higher rate for PA-6 compared with PP. It is also observed that the decrease begins with PA-6. At longer exposure time, the dimensionless MFI of both homopolymers decreases more rapidly. The drop is more pronounced for PP than PA-6, meaning that the degradation rate of PP is higher than that of PA6 for long exposure times. Indeed, PP is a nonabsorbing polymer under irradiation at $\lambda > 300$ nm.[18] The photooxidative degradation involves the absorption of UV light by chromophoric defects that are present in the polymer and formed during the processing of the samples. However, the photooxidation mechanism of PA-6 involves the direct absorption of UV light in the range of 300–340 nm by the NH—(CO) - chromophore, leading to the scission of C—N bands.[15] This explains why photooxidation starts primarily in PA-6 rather than PP. In addition, the tertiary carbon radicals formed during photooxidation of PP are characterized by a very high reactivity.[6]

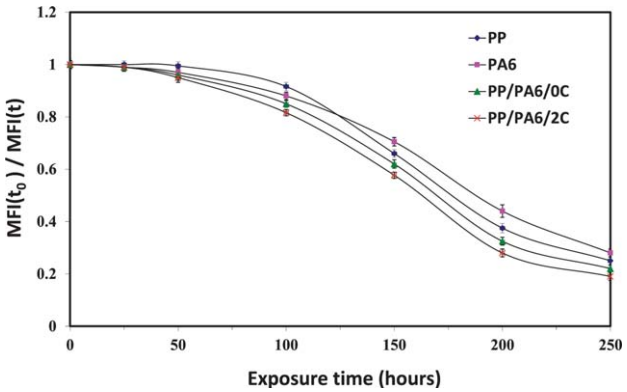

Figure 5. Dimensionless MFI of PP, PA-6, PP/PA-6/0C, and PP/PA-6/2C as a function of exposure time in artificial weathering. [Color figure can be viewed in the online issue, which is available at wileyonlinelibrary.com.]

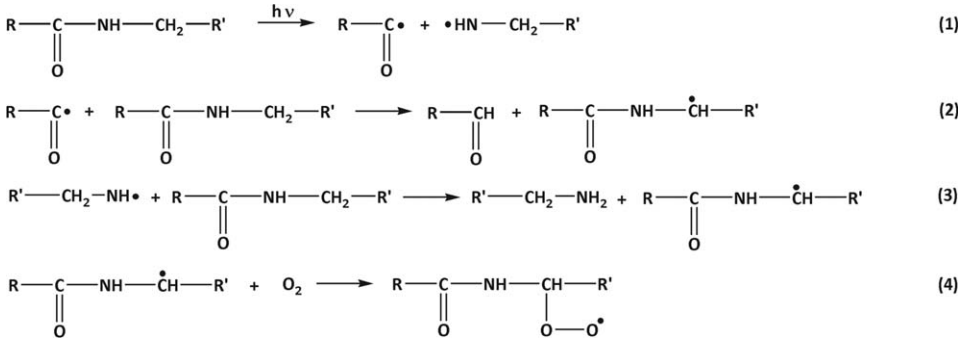

Scheme 1. Possible mechanism of formation of primary oxygenated radicals in PA-6 under photooxidation.[21]

For PP/PA-6 blends, the uncompatibilized samples exhibit approximately the same behavior of PA-6 up to 100 h of irradiation. For longer times of irradiation, the dimensionless MFI values of the blends are below the values measured for the two homopolymers, meaning that the photooxidation rate of the uncompatibilized blends is higher than that of the two components separately for long times of exposure. This phenomenon was also reported by Therias *et al.*[15,21] with polyethylene/polyamide-6 blends and by Waldman *et al.*[6] with polypropylene/polystyrene blends. They suggested that the oxygenated radicals that are produced by oxidation of one component can initiate the oxidation of the other one, leading to an increase of its photooxidation rate, and consequently the increase of the overall degradation rate of the blend. Thereby, it may be suggested that the photooxidation in PP/PA-6 blends starts in PA-6 as described in Scheme 1,[21] since it can directly absorb the UV light in the range 300–340 nm. The primary oxygenated radicals formed can initiate chain oxidation of PP leading to higher photooxidation rate compared to the neat polymer. Furthermore, the addition of PP-*g*-MA to PP/PA-6 blends increases slightly their dimensionless MFI and consequently their photooxidation rate at long exposure time. This may be explained by the fact that the compatibilizer increases the interaction between the different domains of the blend,[6] and thus, enhancing the interactions between the oxygenated radicals that are produced by oxidation of each component leading to higher degradation rate of the blend. In addition, the compatibilizer can participate in the initiation of the degradation reactions due to its lower stability compared with polypropylene. Indeed, according to the literature,[17,22] PP-*g*-MA contains groups that are more susceptible to photooxidation than PP. Moreover, Waldman *et al.*[6] attributed the higher photodegradation rate of PP/PS blends compatibilized with styrene-butadiene-styrene copolymer compared with the uncomptibilized ones to the presence of unsaturated C=C bonds in the butadiene comonomer, which can further react with oxygen, accelerating the degradation cycle.

Tensile Measurements

The effects of photooxidation on mechanical properties of polymer materials are of major importance in most product applications. It is generally believed that chain scission reactions occurring during photooxidation are directly related to mechanical failure.[23] The dimensionless stresses at break of all investigated samples reported as a function of the irradiation time are shown in Figure 6(a). The dimensionless values are calculated by dividing the values of stress at break at a given irradiation time [$SB_{(t)}$] by the corresponding values before exposure [$SB_{(to)}$]. This means that the extent of degradation increases also with the decrease of the dimensionless stress at break. It can be noted that the two homopolymers PP and PA-6 exhibit a slight decay of the stress at break up to 100 h of exposure with a slightly higher rate for PA-6 compared with PP. At higher exposure time, the stress at break of both homopolymers decreases more rapidly, however the decrease is more pronounced in PP than in PA-6.

For the uncompatibilized PP/PA-6 blends, the dimensionless stress at break values are approximately similar to those of PA-6 for short exposure times and below the values corresponding to both components for long irradiation times. Similar trend is

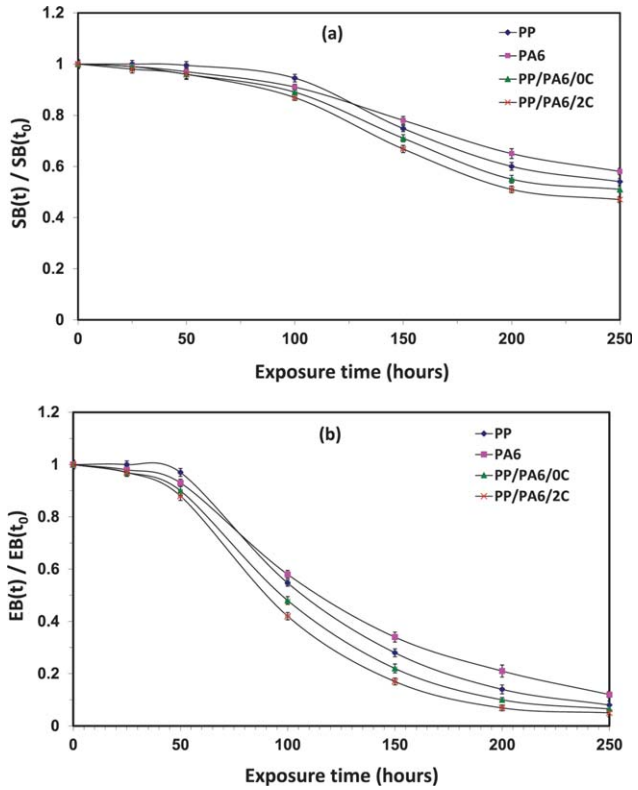

Figure 6. Dimensionless: (a) stress at break and (b) elongation at break of PP, PA-6, PP/PA-6/0C, and PP/PA-6/2C as a function of exposure time in artificial weathering. [Color figure can be viewed in the online issue, which is available at wileyonlinelibrary.com.]

Table II. The Half Time Values of Elongation at Break of PP, PA-6, PP/PA-6/0C, and PP/PA-6/2C

Sample designation	HLT (h)
PP	108
PA-6	115
PP/PA-6/0C	98
PP/PA-6/2C	90

observed for the compatibilized blend, however with a slightly higher decrease of stress at break compared with the uncompatibilized ones after 100 h.

The dimensionless elongation at break of all the investigated samples calculated with the same method as those of stress at break are illustrated in Figure 6(b). The results obtained show similar behavior of the samples as observed in the stress at break measurements, however with a higher rate of decrease of the elongation at break. Indeed, the elongation at break is more sensitive to the structural and morphological variations of the materials occurring during the aging process.[15] Half-life time (HLT) is a very important parameter when studying the durability of polymers. HLT may be considered as the maximum duration for which the samples can still be used. The HLT values of all samples are reported in Table II. This value for the uncompatibilized blend is lower than that of the neat homopolymers PP and PA6. In addition, the incorporation of 2 wt % of the compatibilizer decreases the HLT value of the blends by about 9%.

Table III. Melting Temperature (T_m) and Crystallinity Index (X_c) Measured by DSC of PP, PA-6, PP/PA-6/0C, and PP/PA-6/2C Blends Before Exposure and After 250 h in Artificial Weathering

Samples	Exposure Time (h)	T_m (°C)		X_c (%)	
		PP	PA-6	PP	PA-6
PP	0	166	-	39	-
	250	159	-	45	-
PA-6	0	-	225	-	31
	250	-	219	-	36
PP/PA-6/0C	0	165	223	42	27
	250	157	217	49	33
PP/PA-6/2C	0	166	224	41	29
	250	157	217	50	36

Thermal Properties

DSC data of PP, PA-6, PP/PA-6/0C, and PP/PA-6/2C blends are presented in Table III before and after 150 and 250 h of exposure to accelerated UV test. Before exposure, it is observed that the crystallinity index of PA-6 in the blend is slightly decreased compared with that of the neat polymer. This behavior may be related to the diluent effect of the molten PP component when the minor PA-6 phase crystallizes.[11] However, the crystallinity index (X_c) of PP in the blends is higher than the pure PP one. This effect is higher in the blends without compatibilizer and it is related to the nucleating activity of the PA-6 component in the crystallization of the PP matrix.[11,24] After exposure, an increase in the degree of crystallinity is observed for PP and PA-6 either as neat polymers or as components in the blends. In

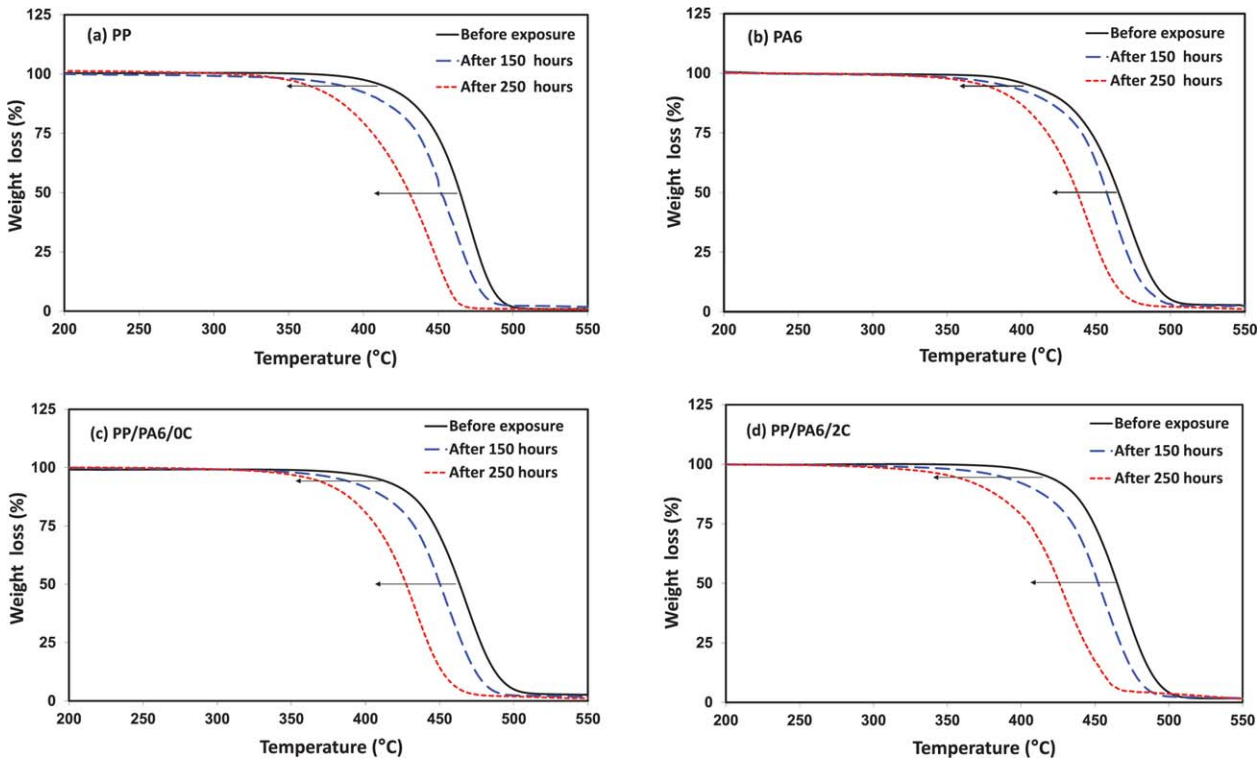

Figure 7. TGA curves of: (a) PP, (b) PA-6, (c) PP/PA-6/0C, and (d) PP/PA-6/2C before exposure and after 150 and 250 h in artificial weathering. [Color figure can be viewed in the online issue, which is available at wileyonlinelibrary.com.]

Table IV. The Decomposition Temperatures at 5 and 50% Weight Loss ($T_{5\%}$, $T_{50\%}$) and the Char Yard at 550°C of PP, PA-6, PP/PA-6/0C, and PP/PA-6/2C Blends as a Function of UV Exposure Time

Samples	Exposure time (h)	$T_{5\%}$ (°C)	$T_{50\%}$ (°C)	Char yard at 550°C (%)
PP	0	413	464	0.6
	150	387	451	0.8
	250	365 (−48)	430 (−34)	0.6
PA-6	0	405	465	1.4
	150	388	457	1.3
	250	374 (−31)	437 (−28)	1.2
PP/PA-6/0C	0	409	463	1.4
	150	384	450	1.3
	250	360 (−49)	427 (−36)	1.2
PP/PA-6/2C	0	413	464	1.2
	150	384	451	1.2
	250	352 (−61)	424 (−40)	1.2

general, the crystallinity is increased due to chain scission, with the consequence segregation of entangled molecule segments and cross-links in the amorphous regions that were not able to crystallize during the original crystallization process. These free segments can reorganize themselves in a crystalline phase, with an appreciable mobility leading to an increase of the degree of crystallinity.[25]

For the melting temperature (T_m), the results obtained show a decrease of the corresponding values of PP and PA-6 either as neat polymers or as components in the blends after exposure to UV light. This may be due to reduction of the molar mass resulting from polymer chain scission in accordance with MFI data.

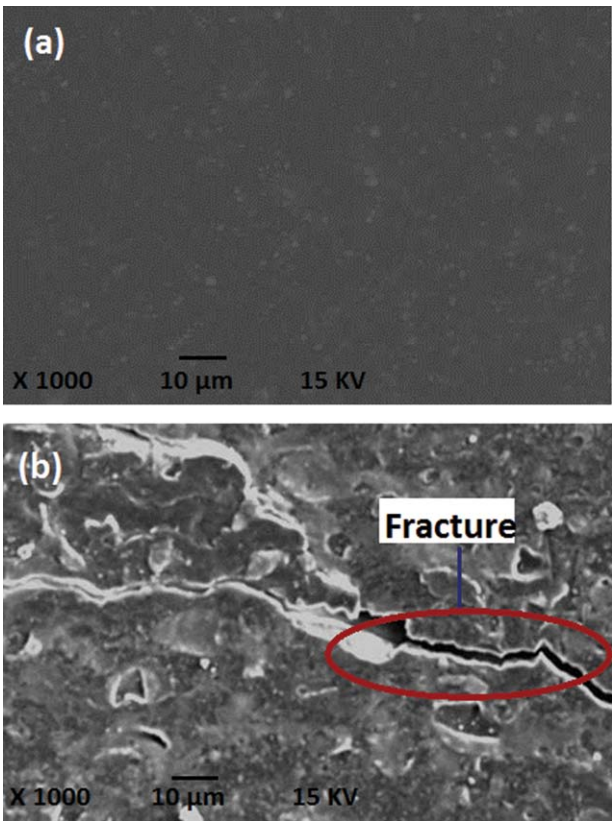

Figure 8. SEM micrographs of fractured surface for PP: (a) before exposure and (b) after 250 h in artificial weathering. [Color figure can be viewed in the online issue, which is available at wileyonlinelibrary.com.]

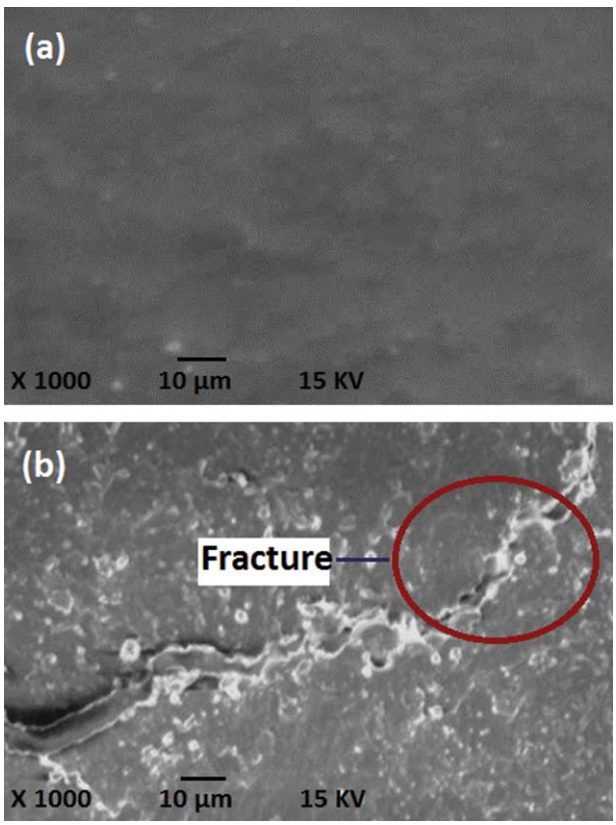

Figure 9. SEM micrographs of fractured surface for PA-6: (a) before exposure and (b) after 250 h in artificial weathering. [Color figure can be viewed in the online issue, which is available at wileyonlinelibrary.com.]

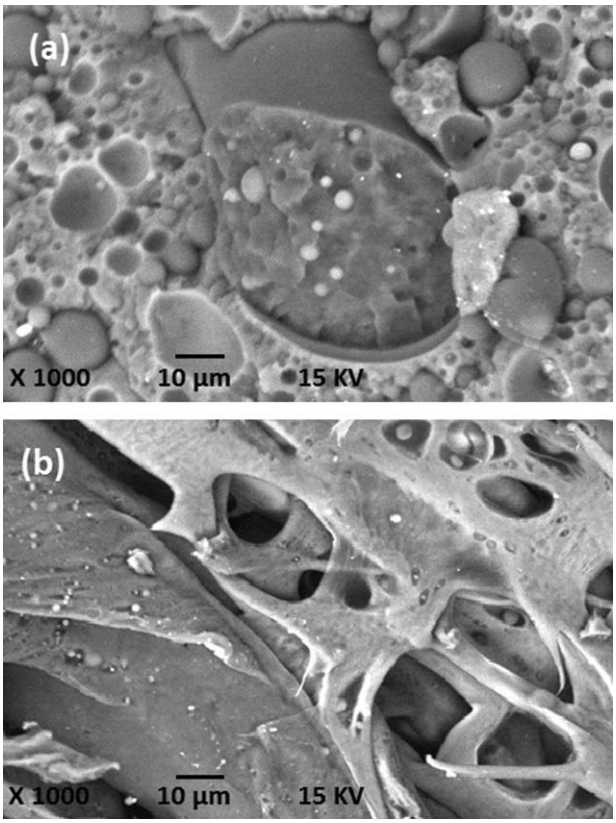

Figure 10. SEM micrographs of fractured surface for PP/PA-6/0C: (a) before exposure and (b) after 250 h in artificial weathering.

TG thermograms of PP, PA-6, PP/PA-6/0C, and PP/PA-6/2C blends recorded in nitrogen atmosphere are shown in Figure 7(a–d), respectively, before and after 150 and 250 h of exposure to accelerated artificial weathering. In addition, Table IV reports the values of ($T_{5\%}$) and ($T_{50\%}$) determined from TGA curves, that is, the temperatures at which 5 and 50% of the total mass are lost. These temperatures provide a good idea of the thermal stability. Before exposure, an increase of the thermal stability of the compatibilized blends is observed compared to the uncompatibilized ones. Indeed, the incorporation of PP-*g*-MA to the blend lead to the increase of $T_{5\%}$ by 4°C passing from 409°C for the uncompatibilized blends to 413°C for the compatibilized ones. Similar results were reported by Roeder *et al.*[26] After exposure, the results reveal a decrease of the thermal stability of all samples: PP, PA-6, PP/PA-6/0C, and PP/PA-6/2C owing to photooxidative degradation. The results show also a higher thermal degradation of PP compared with PA-6 for long times of exposure. Indeed, $T_{5\%}$ of PP falls from 413°C before exposure to 387 and 365°C after 150 and 250 h, respectively. This presents a decrease of 26–48°C. This effect is less pronounced for PA-6, where $T_{5\%}$ decreases from 405°C before exposure to 388 and 374°C after 150 and 250 h, respectively, representing a decrease of 17–31°C.

Figure 7 exhibits a single step of degradation of PP/PA-6 blends. Similar behavior is reported in the literature.[26] One could notice also that the addition of PP-*g*-MA increases the rate of thermal degradation of the blends after exposure. In fact, $T_{5\%}$ of PP/PA-6/0C blend is reduced by 25–49°C passing from 409°C before exposure to 384 and 360°C after 150 and 250 h, respectively. However, $T_{5\%}$ of PP/PA-6/2C decreases by 29–61°C passing from 413°C before exposure to 384 and 352°C after 150 and 250 h of irradiation, respectively.

Similar trend is observed with the degradation temperature at 50% weight loss ($T_{50\%}$) for all the samples. These results are consistent with those obtained by MFI and tensile test, indicating that the compatibilizer acts as thermal degradation promoter at long UV exposure time.

Morphology by SEM

Figure 8(a,b) shows SEM micrographs of the cryo-fractured surfaces of PP before and after 250 h of accelerated weathering exposure. As observed in Figure 8(a), the surface of PP shows a regular and smooth surface before irradiation. After 250 h of exposure, it is observed in Figure 8(b), that the fractured surface becomes rough and is characterized by the formation of cracks and fractures. The surface damages are formed spontaneously during UV exposure as a result of the surface layers, which lead to shrinkage.[27] Similar effects are observed for PA-6 as shown in Figure 9(a,b) before and after UV exposure, however less severe damage is revealed compared with PP after 250 h. This is consistent with the mechanical and MFI results, which showed higher degradation rate of PP compared with PA-6 for high exposure times, although the photooxidation starts primarily in PA-6.

Figure 10(a,b) shows SEM micrographs of cryo-fractured surfaces of PP/PA-6/0C blend before and after 250 h of exposure to artificial accelerating weathering, respectively. From Figure 10(a), it

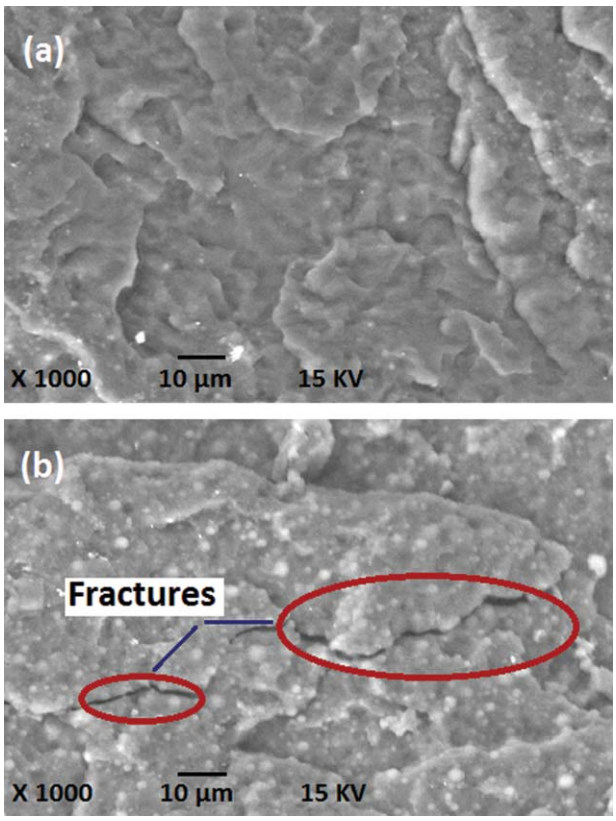

Figure 11. SEM micrographs of fractured surface for PP/PA-6/2C: (a) before exposure and (b) after 250 h in artificial weathering. [Color figure can be viewed in the online issue, which is available at wileyonlinelibrary.com.]

can be observed that the morphology shows irregularly shaped and large domains of PA-6 dispersed in PP matrix due to the poor interfacial adhesion between them. Similar results have been reported in literature.[28] After 250 h of exposure as shown in Figure 10(b), the morphology of the blend exhibits a severe damage resulting from UV degradation. However, the non-irradiated compatibilized PP/PA-6 blend as observed in Figure 11(a) reveals homogeneous phase structures in which the PA-6 particles are embedded with the PP matrix. Indeed, the addition of the compatibilizer improved the dispersion and particle size distribution of the PA-6 phase within the PP matrix. As suggested by Roeder *et al.*,[29] the improved morphology of PP/PA-6/PP-*g*-MA blend results from the formation of an interfacial copolymer. After 250 h of UV irradiation, the morphology of the compatibilized PP/PA-6 blend exhibits the formation of many fractures indicating the occurrence of photooxidative degradation [Figure 11(b)].

CONCLUSION

This work was devoted to study the influence of artificial weathering on the chemical structure and the properties of PP/PA-6 (70/30 wt %) blends compatibilized with PP-*g*-MA. FTIR analysis of the chemical structure of the compatibilized and uncompatibilized blends after exposure to UV light showed the formation of photoproducts corresponding to both components. The MFI and mechanical results obtained reveal that the photooxidation starts in the PA-6 phase. The degradation rate of the uncompatibilized blends is higher than that of both homopolymers at long exposure times. The addition of PP-*g*-MA increases slightly their photooxidation rate. UV exposure increases the crystallinity index and decreases the melting temperature of PP and PA-6 either as neat homopolymers or as components in the blends. SEM micrographs of the cryo-fractured surfaces of the samples showed the formation of cracks and fractures after UV irradiation.

The overall results suggest that the photooxidation in PP/PA-6 blends starts in PA-6 phase initiating chain oxidation of PP. The photooxidation of the two phases occurs simultaneously due to the interactions between the photoproducts of both components, increasing the degradation rate of the blend. The compatibilizer acts as a photooxidation promoter in PP/PA-6 blends. Accordingly, to improve the durability of these blends, it is necessary to prevent them against UV degradation by optimizing the quantity and quality of UV stabilizer to be used.

ACKNOWLEDGMENTS

The authors are grateful to the National Company of Electrical Appliances (INJELEC) and the National Center of Technology and Consulting (CNTC), Algeria for their supports in the realization of this research work. The authors wish to extend their gratitude to Mr Ameziani and Dr Omar Arous for their help in the experimental work.

REFERENCES

1. Zhou, X.; Zhang, P.; Jiang, X.; Rao, G. *Vib. Spectrosc.* **2009**, *49*, 17.
2. Afshari, M.; Kotek, R.; Haghighat Kish, M.; Nazock Dast, H.; Gupta, B. S. *Polymer* **2002**, *43*, 1331.
3. Lee, J-D.; Yang, S. M. *Polym. Eng. Sci.* **1995**, *35*, 1821.
4. Zaidi, L.; Kaci, M.; Bruzaud, S.; Bourmaud, A.; Grohens, Y. *Polym. Degrad. Stab.* **2010**, *95*, 1751.
5. Singh, B.; Sharma, N. *Polym. Degrad. Stab.* **2008**, *93*, 561.
6. Waldman, W. R.; De Paoli, M.-A. *Polym. Degrad. Stab.* **2008**, *93*, 273.
7. Bate, D. M.; Lehrle, R. S. *Polym. Degrad. Stab.* **1998**, *62*, 57.
8. Tzankova Dintcheva, N.; Filippone, G.; La Mantia, F. P.; Acierno, D. *Polym. Degrad. Stab.* **2010**, *95*, 527.
9. Pospisil, J.; Horak, Z.; Krulis, Z.; Nespurek, S.; Kuroda, S.-I. *Polym. Degrad. Stab.* **1999**, *65*, 405.
10. Sathe, S. N.; Devi, S.; Rao, G. S. S.; Rao, K. V. *J. Appl. Polym. Sci.* **1996**, *61*, 97.
11. Compoy, I.; Arribas, J. M.; Zaporta, M. A. M.; Marco, C.; Gomez, M. A.; Fatou, J. G. E. *Polym. J.* **1995**, *31*, 475.
12. Marco, C.; Ellis, G.; Gomez, M. A.; Fatou, J. G.; Arribas, J. M.; Compoy, I.; Fontecha, A. *J. Appl. Polym. Sci.* **1997**, *65*, 2665.
13. Jafari, S. H.; Gupta, A. K. *J. Appl. Polym. Sci.* **1999**, *71*, 1153.
14. Potente, H.; Bastian, M.; Bergemann, K.; Senge, M.; Scheel, G.; Winkelmann, T. H. *Polym. Eng. Sci.* **2001**, *41*, 222.
15. Therias, S.; Tzankova Dintcheva, N.; Gardette, J. L.; La Mantia, F. P. *Polym. Degrad. Stab.* **2010**, *95*, 522.
16. Mouffok, S.; Kaci, M.; Peuvler-Disdier, E.; Aliouche, D. *Macromol. Symp.* **2012**, 321–322, *40*.
17. Al-Shabanat, M. *Int. J. Chem.* **2011**, *3*, 129.
18. Rivaton, A.; Serre, F.; Gardette, J. L. *Polym. Degrad. Stab.* **1998**, *62*, 127.
19. Lemaire, J.; Gardette, J. L.; Rivaton, A.; Roger, A. *Polym. Degrad. Stab.* **1986**, *15*, 1.
20. Kaci, M.; Djidjelli, H.; Boukedami, T. *Polym. Bull.* **2008**, *60*, 387.
21. Nocilla, M. A.; La Mantia, F. P. *Polym. Degrad. Stab.* **1990**, *29*, 331.
22. Abu-Sharkh, B. F.; Hamid, H. *Polym. Degrad. Stab.* **2004**, *85*, 967.
23. Duarte, F. M.; Botelho, G.; Machado, A. V. *Polym. Test.* **2006**, *25*, 91.
24. Pigłowskia, J.; Gancarz, I.; Wlaz′lak, M.; Kammer, H.-W. *Polymer* **2000**, *41*, 6813.
25. Larena, A.; Jiménez De Ochoa, S.; Domınguez, F. *Polym. Degrad. Stab.* **2006**, *91*, 940.
26. Roeder, J.; Oliveira, R. V. B.; Becker, D.; Gonçalves, M. W.; Soldi, V.; Pires, A. T. N. *Polym. Degrad. Stab.* **2005**, *90*, 481.
27. Rabello, M. S.; White, J. R. *J. Appl. Polym. Sci.* **1997**, *64*, 2505.
28. Yoon, B. S.; Joang, J. Y.; Suh, M. H.; Lee, Y. M.; Lee, S. H. *Polym. Comp.* **1997**, *18*, 757.
29. Roeder, J.; Oliveira, R. V. B.; Gonçalves, M. C.; Soldi, V.; Pires, A. T. N. *Polym. Test.* **2002**, *21*, 815.